Acta Crystallographica Section F
Structural Biology Communications
ISSN 2053-230X

Purification, crystallization and phase determination of the DR1998 haem *b* catalase from *Deinococcus radiodurans*

Patrícia T. Borges,‡ Cecília S. Miranda,‡ Sandra P. Santos, João N. Carita, Carlos Frazão and Célia V. Romão*

Instituto de Tecnologia Química e Biológica, Universidade Nova de Lisboa, Avenida da República, Estação Agronómica Nacional, 2780-157 Oeiras, Portugal

‡ These authors contributed equally to this work.

Correspondence e-mail: cmromao@itqb.unl.pt

Received 26 February 2014
Accepted 4 April 2014

The protective mechanisms of *Deinococcus radiodurans* against primary reactive oxygen species involve nonenzymatic scavengers and a powerful enzymatic antioxidant system including catalases, peroxidases and superoxide dismutases that prevents oxidative damage. Catalase is an enzyme that is responsible for the conversion of H_2O_2 to O_2 and H_2O, protecting the organism from the oxidative effect of H_2O_2. This study reports the purification and crystallization of the DR1998 catalase from *D. radiodurans*. The crystals diffracted to 2.6 Å resolution and belonged to space group $C222_1$, with unit-cell parameters a = 97.33, b = 311.88, c = 145.63 Å, suggesting that they contain four molecules per asymmetric unit. The initial phases were determined by molecular replacement and the obtained solution shows the typical catalase quaternary structure. A preliminary model of the protein structure has been built and refinement is currently in progress.

1. Introduction

The bacterium *Deinococcus radiodurans* has significant resistance to ionizing and ultraviolet radiation or desiccation. The organism is able to deal with the side effects of these conditions, namely the intracellular oxidative stress that is incurred by an increase in the formation of reactive oxygen species (ROS; Cox & Battista, 2005; Slade & Radman, 2011; White *et al.*, 1999). ROS can damage proteins, lipids, nucleic acids and carbohydrates and can induce double-strand DNA breaks in the bacterial genome (Brawn & Fridovich, 1981).

The protective mechanism of *D. radiodurans* against oxidative damage involves nonenzymatic scavengers such as divalent manganese complexes and carotenoids and a powerful enzymatic antioxidant system including superoxide dismutases, catalases and peroxidases against primary ROS such as superoxide radical ($O_2^{\bullet-}$) and hydrogen peroxide (H_2O_2) (Culotta & Daly, 2013; Slade & Radman, 2011; Tian & Hua, 2010; Fridovich, 1978; Chou & Tan, 1990; Lipton *et al.*, 2002). Catalases (EC 1.11.1.6) from many species are known to be tetrameric enzymes that catalyze the disproportionation of H_2O_2 to O_2 and H_2O, and can be classified based on their catalytic metal centre as haem, nonhaem or Mn-containing catalases. The group of haem-containing catalases includes monofunctional catalases and bifunctional catalase-peroxidases which have both catalase and peroxidase activities (Chelikani *et al.*, 2004; Maté *et al.*, 2006; Zamocky *et al.*, 2008).

An analysis of the *D. radiodurans* genome indicated that this organism encodes three catalases: DR1998, DRA0259 and DRA0146 (White *et al.*, 1999; Makarova *et al.*, 2001). Catalase activity has been reported in several studies of *D. radiodurans*. An increase in the catalase activity has been observed in the stationary phase from growth of *D. radiodurans* in the presence of manganese when compared with a control (Chou & Tan, 1990); an increase in the total catalase activity in bacterial cultures pretreated with 10 m*M* H_2O_2 was also observed, and it is interesting to note that under this condition the bacterial cultures were more resistant to the lethal effects of UV and γ radiation (Wang & Schellhorn, 1995). A knockout mutant deficient in catalase was observed to be more sensitive to ionizing radiation than wild-type bacteria (Markillie *et al.*, 1999). Although all of these studies suggest an essential role of the

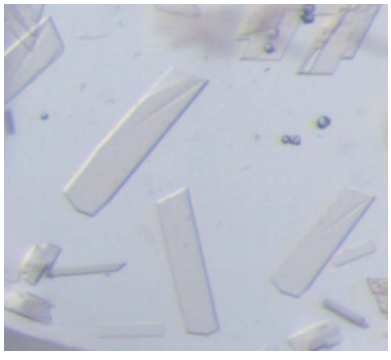

antioxidant enzymes in this organism, the only such enzyme that has been characterized from *D. radiodurans* is DR1998, which is classified as a monofunctional haem-containing catalase, since peroxidase activity is absent (Kobayashi *et al.*, 2006), and is constitutively expressed (Lipton *et al.*, 2002).

In this study, we describe the purification of the DR1998 catalase isolated directly from *D. radiodurans*, its crystallization, diffraction data collection to 2.6 Å resolution and a preliminary crystallographic analysis that confirmed its oligomerization as homotetrameric, similar to other monofunctional catalases.

2. Materials and methods

2.1. Bacterial growth and protein purification

D. radiodurans was grown at 303 K on M53 medium until the optical density at 600 nm reached 2.0. Cells obtained from 300 l of culture were harvested, resuspended in 20 m*M* Tris–HCl pH 7.2 and disrupted in a French press at 62 MPa. After ultracentrifugation (182 000*g*, 6 h 30 min), the soluble fraction was dialysed overnight against 20 m*M* Tris–HCl pH 7.2 at 277 K.

All purification procedures were performed in 20 m*M* Tris–HCl pH 7.2 at 277 K using an ÄKTAprime (GE Healthcare). Protein concentration was performed in a Diaflo ultrafiltration device (Amicon) using YM10 membrane. DR1998 catalase was purified from the soluble fraction in three consecutive anionic chromatography steps, firstly a DEAE-Fast Flow column (10 ml min^{-1}; XK 50/30, GE Healthcare) and secondly a Q-Sepharose HP column (2 ml min^{-1}; XK 26/10, GE Healthcare), both using a linear gradient from 0 to 1 *M* NaCl. Finally, a HiTrap Q-HP column (1.5 ml min^{-1}; GE Healthcare) was used with a linear gradient from 0 to 1 *M* sodium acetate. Between each chromatography step, the catalase fraction was dialysed; it always eluted at ∼0.6 *M* ionic strength.

Protein purity was confirmed by SDS–PAGE (Fig. 1*a*). The protein band was analysed by N-terminal sequencing. The obtained sequence (VQGVGGPR) was compared with the *D. radiodurans* genome database and the protein was identified as DR1998 catalase. The molecular mass deduced from its amino-acid sequence is 60 513 Da. The UV–visible absorption spectrum of the catalase displayed absorption maxima typical of a haem protein, with the Soret band at 406 nm, two broad bands at 503 and 538 nm, and a band at 625 nm indicating a high-spin haem (Fig. 1*b*).

Table 1
Diffraction data-collection and processing parameters.

Values in parentheses are for the highest resolution shell.

Beamline	ID29, ESRF
Detector	PILATUS 6M
Wavelength (Å)	0.826560
Data-processing software	*XDS*
Space group	$C222_1$
Unit-cell parameters (Å)	a = 97.33, b = 311.88, c = 145.63
Resolution (Å)	78.3–2.60 (2.76–2.60)
No. of observations	352748 (48698)
Unique reflections	68047 (10656)
Completeness (%)	99.3 (97.5)
Multiplicity	5.2 (4.6)
Mosaicity (°)	0.049
$CC_{1/2}$† (%)	97.1 (75.4)
R_{merge}‡ (%)	30.8 (83.8)
R_{meas}§ (%)	34.3 (96.2)
$R_{p.i.m.}$¶ (%)	12.0 (27.4)
$\langle I/\sigma(I)\rangle$	5.3 (1.7)
Wilson B factor (Å^2)	25
No. of molecules in asymmetric unit	4
V_M (Å^3 Da^{-1})	2.28
Estimated crystal solvent content (%)	46

† $CC_{1/2}$ is the percentage of correlation between intensities from random half-data sets (Karplus & Diederichs, 2012). ‡ $R_{merge} = \sum_{hkl}\sum_i |I_i(hkl) - \langle I(hkl)\rangle| / \sum_{hkl}\sum_i I_i(hkl)$, where $I_i(hkl)$ is the observed intensity and $\langle I(hkl)\rangle$ is the average intensity of multiple observations of symmetry-related reflections (Arndt *et al.*, 1968). § $R_{meas} = \sum_{hkl}\{N(hkl)/[N(hkl)-1]\}^{1/2}\sum_i |I_i(hkl) - \langle I(hkl)\rangle| / \sum_{hkl}\sum_i I_i(hkl)$, where $N(hkl)$ is the data multiplicity, $I_i(hkl)$ is the observed intensity and $\langle I(hkl)\rangle$ is the average intensity of multiple observations of symmetry-related reflections. It is an indicator of the agreement between symmetry-related observations (Diederichs & Karplus, 1997). ¶ $R_{p.i.m.} = \sum_{hkl}\{1/[N(hkl)-1]\}^{1/2}\sum_i |I_i(hkl) - \langle I(hkl)\rangle| / \sum_{hkl}\sum_i I_i(hkl)$, where $N(hkl)$ is the data multiplicity, $I_i(hkl)$ is the observed intensity and $\langle I(hkl)\rangle$ is the average intensity of multiple observations of symmetry-related reflections. It is an indicator of the precision of the final merged and averaged data set (Weiss, 2001).

2.2. Crystallization and cryoprotection

Crystallization conditions were screened with a nanodrop crystallization robot (Cartesian, Genomic Solutions) using Structure Screen I and II (Molecular Dimensions) at 293 K. Crystals were obtained in condition B3 consisting of 0.2 *M* magnesium acetate, 0.1 *M* sodium

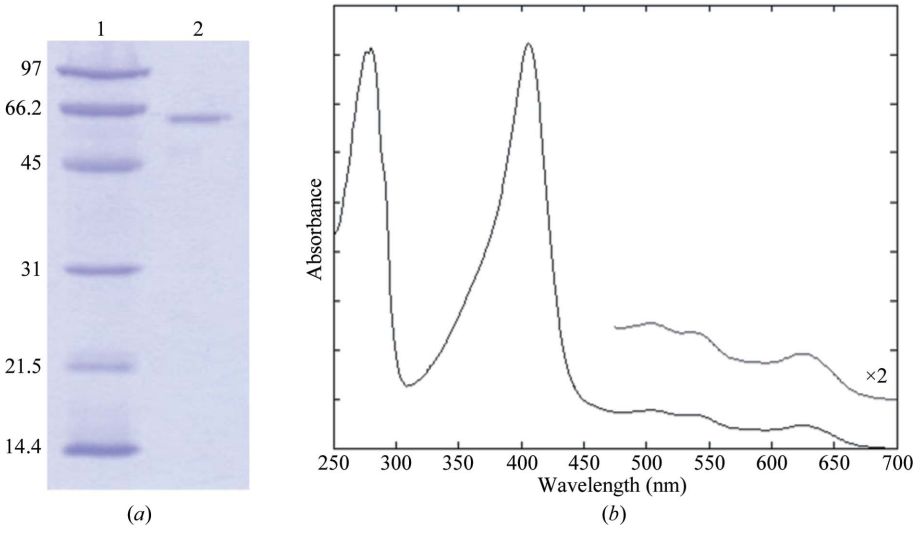

(*a*) (*b*)

Figure 1
(*a*) SDS–PAGE. Lane 1, low-molecular-weight markers (kDa); lane 2, DR1998 catalase protein eluted from HiTrap Q-HP. (*b*) UV–Vis absorption spectrum of DR1998 catalase indicating the presence of a *b*-type haem.

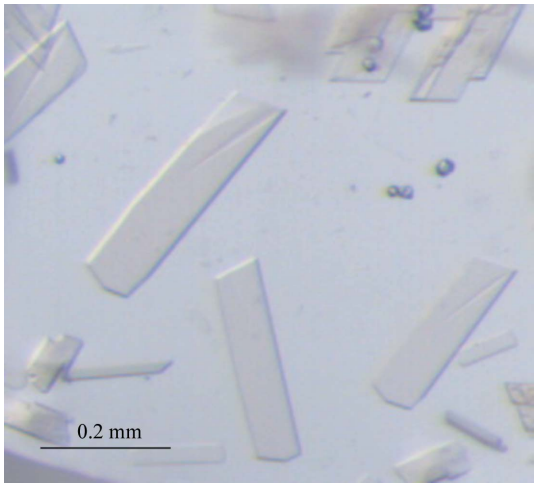

Figure 2
Brown crystals of DR1998 catalase grown in 0.2 *M* magnesium acetate, 0.1 *M* sodium cacodylate pH 6.5, 20% PEG 8000.

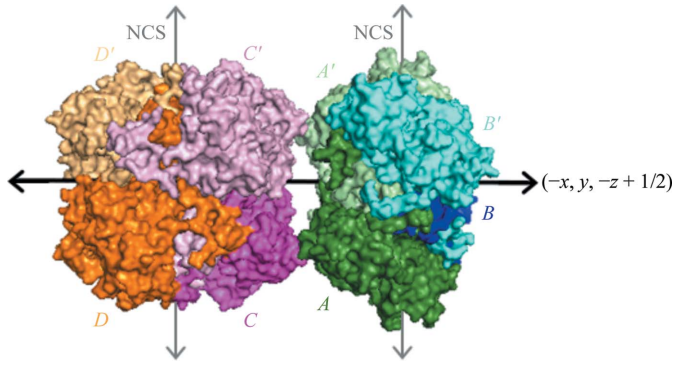

Figure 3
Solvent-accessible molecular-surface representation of the molecular-replacement solution: *A*, *B*, *C* and *D* (in darker colours) correspond to the DR1998 asymmetric unit and *A*′, *B*′, *C*′ and *D*′ (in lighter colours) correspond to the crystallographic image from the operation $(-x, y, -z + 1/2)$. This symmetry operation builds up the typical catalase oligomers (*ABA*′*B*′) and (*CDC*′*D*′), each with 222 point-group symmetry, upon combination of the crystallographic C_2 symmetry with local twofold symmetry axes. Directions *x* and *y* are in the plane of the paper and direction *z* is perpendicular to this plane.

cacodylate pH 6.5, 20% PEG 8000. Additional optimization experiments were carried out in order to improve the crystal quality and size. Different modifications of the initial condition were tested using the hanging-drop method by mixing 1.0 µl native protein as purified (12 mg ml^{-1} in 20 m*M* Tris–HCl pH 7.2, 0.6 *M* NaCl) with 1.0 µl reservoir solution (Fig. 2). Catalase crystals were cryoprotected using the reservoir solution supplemented with 25% glycerol prior to flash-cooling in liquid nitrogen.

2.3. Data collection and processing

Several crystals were subjected to X-ray radiation under a 100 K nitrogen stream and diffraction was barely visible. Nevertheless, one data set was collected on beamline ID29 of the European Synchrotron Radiation Facility (ESRF), Grenoble, France. Diffraction images were collected using a PILATUS 6M detector. A total of 1400 oscillation images were recorded using two passes of 0.1° 0.08 s exposures over a total crystal rotation of 140° at a crystal-to-detector distance of 686.46 mm. Images were integrated and the intensities produced were scaled with *XDS* (Kabsch, 2010). Data-collection details and processing statistics are listed in Table 1.

3. Results and discussion

DR1998 protein crystals produced very weak diffraction and the best diffracting crystal obtained to date gave individual intensities with a global $\langle I/\sigma(I)\rangle$ of 2.3. With such a low signal-to-noise ratio in the original data, it was not a surprise to obtain an unusually high $R_{\rm merge}$ of 0.308. However, after merging all symmetry-related intensities, with a multiplicity of 5.2, the final merged and averaged data set showed a signal-to-noise ratio $\langle I/\sigma(I)\rangle$ of 5.3 (Table 1).

The crystal belonged to the orthorhombic space group $C222_1$, with unit-cell parameters a = 97.33, b = 311.88, c = 145.63 Å. The distribution of the Matthews coefficient (Matthews, 1968; Kantardjieff & Rupp, 2003) at 2.6 Å resolution indicated a 71% probability of four DR1998 molecules in the asymmetric unit, which corresponded to a calculated solvent content of 46% and a $V_{\rm M}$ of 2.28 Å^3 Da^{-1}. Unexpectedly, the self-rotation distribution did not show the presence of any additional noncrystallographic rotational axes in the asymmetric unit in addition to the three crystallographic twofold axes along the three orthogonal directions.

Since several catalase structures are available in the Protein Data Bank (Berman *et al.*, 2000), attempts were made to solve the phase problem using molecular replacement. A sequence-similarity search using the DR1998 sequence (White *et al.*, 1999) was performed with *FASTA* (Pearson & Lipman, 1988) at the EBI site (http://www.ebi.ac.uk) on available catalase structures. The structure with the highest identity (50%) was the catalase from *Exiguobacterium oxidotolerans* (PDB entry 2j2m; Hara *et al.*, 2007). However, molecular-replacement attempts using the monomer, dimer or tetramer as search models with *Phaser* (McCoy *et al.*, 2007) in the *PHENIX* suite (Adams *et al.*, 2010) were unsuccessful. With the aim of producing a more suitable search model by trying to increase the accuracy of the search fold to reproduce that of DR1998, the program *PDBeFold* (http://www.ebi.ac.uk/msd-srv/ssm/cgi-bin/ssmserver) was used to superpose the six catalase models with highest sequence similarity (50–34%): PDB entries 2j2m from *Exiguobacterium oxidotolerans* (Hara *et al.*, 2007), 1m7s from *Pseudomonas syringae* (Carpena *et al.*, 2003), 1gwe from *Micrococcus luteus* (Murshudov *et al.*, 2002), 1dgf from *Homo sapiens* (Putnam *et al.*, 2000), 2iuf from *Penicillium janthinellum* (Alfonso-Prieto *et al.*, 2007) and 1sy7 from *Neurospora crassa* (Díaz *et al.*, 2004). The ensemble was examined with *Coot* (Emsley & Cowtan, 2004) and nonsuperposed chain segments and most external loops were excluded in order to target only the structurally conserved regions within this set of structures. This time, *Phaser* succeeded in locating four molecules in the asymmetric unit with translation-function *Z*-scores (TFZs) of 20, 35, 47 and 56, which indicate a successful solution (Oeffner *et al.*, 2013). A packing analysis of the solution revealed that the four molecules in the asymmetric unit are arranged as two different dimers (Fig. 3), with twofold NCS axes parallel to directions *x* and *z*, thus explaining why the rotation function did not reveal additional NCS axes. The combination of the two dimers with the crystallographic symmetry generates two independent DR1998 tetramers that display the typical catalase oligimerization architecture. The DR1998 catalase structure is currently under refinement in order to provide insights into the molecular function of this catalase.

This work was supported by grants and fellowships from Fundação para a Ciência e Tecnologia under the following projects: PTDC/

BIA-PRO/100365/2008 (CVR) and PEst-OE/EQB/LA0004/2011. PTB is the recipient of PhD grant SFRH/BD/85106/2012. CSM was supported by a BI fellowship within FCT grant PTDC/BIA-PRO/100365/2008. SPS is the recipient of PhD grant SFRH/BD/78870/2011. CVR is the recipient of grant SFRH/BPD/94050/2013. We thank the staff at ESRF, Grenoble, France for the use of synchrotron radiation.

References

Adams, P. D. *et al.* (2010). *Acta Cryst.* D**66**, 213–221.
Alfonso-Prieto, M., Borovik, A., Carpena, X., Murshudov, G., Melik-Adamyan, W., Fita, I., Rovira, C. & Loewen, P. C. (2007). *J. Am. Chem. Soc.* **129**, 4193–4205.
Arndt, U. W., Crowther, R. A. & Mallett, J. F. (1968). *J. Sci. Instrum.* **1**, 510–516.
Berman, H. M., Westbrook, J., Feng, Z., Gilliland, G., Bhat, T. N., Weissig, H., Shindyalov, I. N. & Bourne, P. E. (2000). *Nucleic Acids Res.* **28**, 235–242.
Brawn, K. & Fridovich, I. (1981). *Arch. Biochem. Biophys.* **206**, 414–419.
Carpena, X., Soriano, M., Klotz, M. G., Duckworth, H. W., Donald, L. J., Melik-Adamyan, W., Fita, I. & Loewen, P. C. (2003). *Proteins*, **50**, 423–436.
Chelikani, P., Fita, I. & Loewen, P. C. (2004). *Cell. Mol. Life Sci.* **61**, 192–208.
Chou, F. I. & Tan, S. T. (1990). *J. Bacteriol.* **172**, 2029–2035.
Cox, M. M. & Battista, J. R. (2005). *Nature Rev. Microbiol.* **3**, 882–892.
Culotta, V. C. & Daly, M. J. (2013). *Antioxid. Redox Signal.* **19**, 933–944.
Díaz, A., Horjales, E., Rudiño-Piñera, E., Arreola, R. & Hansberg, W. (2004). *J. Mol. Biol.* **342**, 971–985.
Diederichs, K. & Karplus, P. A. (1997). *Nature Struct. Biol.* **4**, 269–275.
Emsley, P. & Cowtan, K. (2004). *Acta Cryst.* D**60**, 2126–2132.
Fridovich, I. (1978). *Science*, **201**, 875–880.
Hara, I., Ichise, N., Kojima, K., Kondo, H., Ohgiya, S., Matsuyama, H. & Yumoto, I. (2007). *Biochemistry*, **46**, 11–22.
Kabsch, W. (2010). *Acta Cryst.* D**66**, 125–132.
Kantardjieff, K. A. & Rupp, B. (2003). *Protein Sci.* **12**, 1865–1871.
Karplus, P. A. & Diederichs, K. (2012). *Science*, **336**, 1030–1033.
Kobayashi, I., Tamura, T., Sghaier, H., Narumi, I., Yamaguchi, S., Umeda, K. & Inagaki, K. (2006). *J. Biosci. Bioeng.* **101**, 315–321.
Lipton, M. S. *et al.* (2002). *Proc. Natl Acad. Sci. USA*, **99**, 11049–11054.
Makarova, K. S., Aravind, L., Wolf, Y. I., Tatusov, R. L., Minton, K. W., Koonin, E. V. & Daly, M. J. (2001). *Microbiol. Mol. Biol. Rev.* **65**, 44–79.
Markillie, L. M., Varnum, S. M., Hradecky, P. & Wong, K. K. (1999). *J. Bacteriol.* **181**, 666–669.
Maté, M. J., Murshudov, G., Bravo, J., Melik-Adamyan, W., Loewen, P. C. & Fita, I. (2006). In *Handbook of Metalloproteins*, edited by A. Messerschmidt, R. Huber, T. Poulos & K. Weighardt. Chichester: John Wiley & Sons. doi:10.1002/0470028637.met134.
Matthews, B. W. (1968). *J. Mol. Biol.* **33**, 491–497.
McCoy, A. J., Grosse-Kunstleve, R. W., Adams, P. D., Winn, M. D., Storoni, L. C. & Read, R. J. (2007). *J. Appl. Cryst.* **40**, 658–674.
Murshudov, G. N., Grebenko, A. I., Brannigan, J. A., Antson, A. A., Barynin, V. V., Dodson, G. G., Dauter, Z., Wilson, K. S. & Melik-Adamyan, W. R. (2002). *Acta Cryst.* D**58**, 1972–1982.
Oeffner, R. D., Bunkóczi, G., McCoy, A. J. & Read, R. J. (2013). *Acta Cryst.* D**69**, 2209–2215.
Pearson, W. R. & Lipman, D. J. (1988). *Proc. Natl Acad. Sci. USA*, **85**, 2444–2448.
Putnam, C. D., Arvai, A. S., Bourne, Y. & Tainer, J. A. (2000). *J. Mol. Biol.* **296**, 295–309.
Slade, D. & Radman, M. (2011). *Microbiol. Mol. Biol. Rev.* **75**, 133–191.
Tian, B. & Hua, Y. (2010). *Trends Microbiol.* **18**, 512–520.
Wang, P. & Schellhorn, H. E. (1995). *Can. J. Microbiol.* **41**, 170–176.
Weiss, M. S. (2001). *J. Appl. Cryst.* **34**, 130–135.
White, O. *et al.* (1999). *Science*, **286**, 1571–1577.
Zamocky, M., Furtmüller, P. G. & Obinger, C. (2008). *Antioxid. Redox Signal.* **10**, 1527–1548.